Green Speaker Design
(Part 2: Optimal Use of Transducer Resources)

Wolfgang Klippel, KLIPPEL GmbH, Mendelssohnallee 30, 01277 Dresden, Germany

Green speaker design is a new concept for developing active loudspeaker systems that generate the desired sound output with minimum size, weight, cost and energy. This paper focuses on the optimization of the transducer by exploiting the new opportunities provided by digital signal processing. Nonlinear adaptive control can compensate for the undesired signal distortion, protect the transducer against overload, stabilize the voice coil position and cope with time varying properties of the suspension. The transducer has to provide maximum efficiency of the electro-acoustical conversion and sufficient voltage sensitivity to cope with the amplifier limitations. The potential of the new concept is illustrated using a transducer intended for automotive application.

1 Introduction

Although enclosure and other mechanical and acoustical elements determine the size, shape and weight of the audio product, the electro-acoustical transducer usually limits the voltage sensitivity and efficiency in loudspeaker systems. In small, direct radiating loudspeakers almost 100 % of the electrical power will heat up the voice coil [1]. Doubling the input power is not possible in most professional applications because it would damage the voice coil or it consumes too much energy in mobile applications with limited battery capacity. Voltage sensitivity is a second weakness of the electro-dynamical transducer because the back electromagnetic force (EMF) generated by the voice coil velocity makes it hard to feed electrical energy into the transducer at the fundamental resonance at f_s. Power efficiency and voltage sensitivity are different characteristics, and this becomes obvious when the spectrum $G_w(t)$ of the audio stimulus $w(t)$ is considered in the modeling.

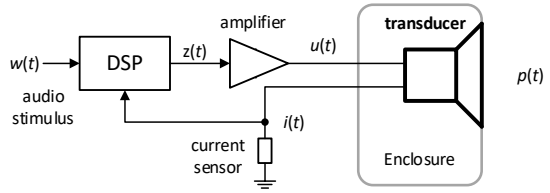

Figure 1: Active loudspeaker system with adaptive, nonlinear control of the transducer based on voltage and current monitoring

A new concept for designing an active loudspeaker system has been presented in the first part of the *Green Speaker Design* [2]. Digital signal processing (DSP) applied to the electrical input signal $u(t)$ of the passive system (transducer + box) as shown in Figure 1 opens up new degrees of freedom in the design of the hardware components. A software solution based on adaptive nonlinear control with current sensing [3] is superior to any hardware solution with respect to

- reducing linear and nonlinear signal distortion [4],
- reliable protection against thermal and mechanical overload [5], [6] and
- stabilization of the voice coil position [7],

while coping with aging, climate and other external influences and generating a desired linear transfer behavior over the life time of the audio device.

This paper continues the discussion on the optimal use of all hardware resources in the first paper [2] but focusses on the transducer. After analyzing consequences for the power amplifier, the potential of the new design concept will be illustrated by slight modification of a loudspeaker intended for a passenger warning system in electric cars.

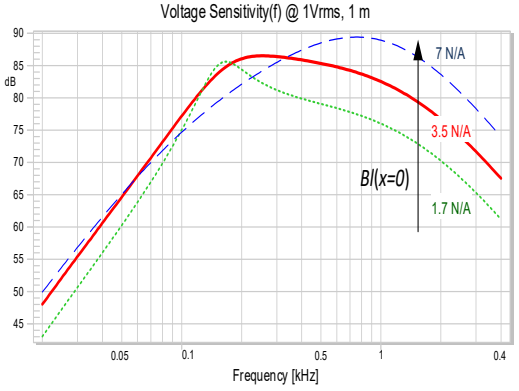

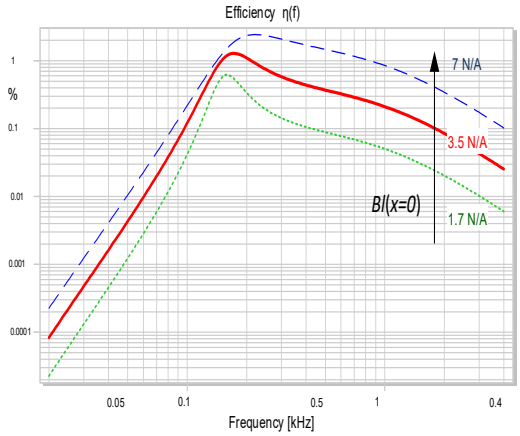

Figure 2: Voltage sensitivity $SPL_{1V,1m}(f)$ and efficiency $\eta(f)$ of an electro-dynamical transducer mounted in a baffle versus frequency f of a single tone stimulus using three different values of the force factor $Bl(x=0)$ at the rest position.

2 Transducer Modeling

Lumped parameter modeling is a convenient basis for modeling transducers used in loudspeakers and other audio devices. The interested reader is referred to the first part [2] where the equivalent circuit and the parameters for the electro-dynamical transducer have been discussed.

This paper here neglects the influences of generator resistance R_g and load impedance $Z_L(f)$ representing the electro-mechanical system (box, passive radiator, panel…) and operates the transducer in an infinite half-space which is usually a baffle. Figure 2 shows the efficiency $\eta(f)$ and voltage sensitivity $SPL_{1V,1m}(f)$ on-axis at distance r_{ref} = 1m of an electro-dynamical loudspeaker mounted in an infinite baffle assuming omnidirectional radiation into the half space for a sinusoidal tone of frequency f and terminal voltage u_{ref} = 1Vrms. The frequency responses of efficiency $\eta(f)$ and voltage sensitivity $SPL_{1V,1m}(f)$ have a similar shape if the motor uses a small magnet that provides a low force factor Bl, as shown for the dotted curves for Bl = 1.7 N/A. For a larger magnet generating a force factor Bl= 7 N/A, the curves are significantly different [9].

The relationship between the lumped transducer parameters and the two important characteristics will be discussed in three main frequency bands in the following chapters.

2.1 Passband

The efficiency $\eta(f)$ is almost constant in the passband of the transducer with $2f_s < f < 5f_s$, where $ka < 1$, the back EMF is not active and the effect of the inductance L_E is negligible. A frequency independent value called passband efficiency η_{PB} is defined as

$$\eta_{PB} = \frac{(Bl)^2}{R_E M_{MS}^2} \frac{\rho_0 S_D^2}{2\pi c} 100\% \qquad (1)$$

using the lumped parameter modeling [2], the density of air ρ_0 and assuming omni-directional radiation into the half-space [8].

The passband efficiency η_{PB} rises with force factor Bl and the effective radiation area S_D but falls with DC resistance R_E and moving mass M_{MS}.

The passband voltage sensitivity can be calculated as the sound pressure level

$$SPL_{PB,u_{ref},r_{ref}} = 20\lg\left(\frac{\rho_0}{2\pi|r_{ref}|}\frac{BlS_D}{R_E M_{MS}}\frac{u_{ref}}{p_0}\right) \qquad (2)$$

generated on-axis at the distance r_{ref}=1m by a defined rms voltage u_{ref} at the transducer terminals. For defining the peak voltage requirement of the amplifier and selecting the transducer with optimum nominal input impedance Z_N, the voltage sensitivity shall be compared at the same reference voltage (e.g. u_{ref}= 1 V_{rms}).

In the passband there is a close relationship between efficiency η_{PB} and voltage sensitivity

$$\begin{aligned} SPL_{PB,u_{ref},r_{ref}} &= 10\lg\left(|H(f,r_{ref})|^2 \frac{Z_N 1W}{p_0}\right) \\ &= 10\lg\left(\frac{\eta_{PB} 1W}{100\%\Pi_0}\frac{Z_N}{R_E}\right) - 8dB \\ &= 10\lg\left(\frac{\eta_{PB}}{100\%}\frac{Z_N}{R_E}\right) + 112dB \end{aligned} \qquad (3)$$

using a particular reference rms voltage $u_{ref} = \sqrt{Z_N 1W}$ (usually 2 or 2.8 V) that generates 1W input power at the nominal impedance Z_N of the device under test (usually 4 or 8 Ohm). Eqs. (2) and (3) also use the reference sound pressure $p_0 = 2\cdot10^{-5}$ Pa and the standard reference power $\Pi_0 = 10^{-12}$ W.

2.2 Fundamental Resonance

The efficiency of the loudspeaker at the fundamental resonance frequency f_s can be calculated by

$$\eta(f_s) = \frac{(Bl)^2 S_D^2 \rho_0 2\pi f_s^2}{\left((Bl)^2 + R_E R_{MS}\right) R_{MS} c}. \qquad (4)$$

For woofers and other similar transducers, where the electrical resistance transformed to the mechanical domain $(Bl)^2 / R_E$ is much larger than the mechanical resistance R_{MS} and the electrical damping dominates the total damping, the efficiency $\eta(f_s)$ is described as

$$\eta(f_s) = \frac{S_D^2 \rho_0 2\pi f_s^2}{R_{MS} c} \qquad (5)$$

and becomes independent of force factor Bl and DC resistance R_E. The small value of the mechanical resistance R_{MS} generates a distinct maximum of the efficiency at resonance ($\eta(f_s) > \eta_{PB}$). However, a high force factor value Bl will reduce the voltage sensitivity at the resonance to

$$SPL_{u_{ref},r_{ref}}(f_s) = 20\lg\left(\frac{\rho_0 f_s S_D}{|r_{ref}|}\frac{u_{ref}}{Bl}\frac{1}{p_0}\right). \qquad (6)$$

Contrary to the passband region where efficiency and voltage sensitivity are rising with the force factor, a low force factor Bl would improve the voltage sensitivity at resonance. That means a subwoofer designed for a narrow audio band close to the fundamental resonance can use a weak motor with a

small force factor Bl and would be the best choice for high efficiency and high voltage sensitivity [10].

2.3 Low Frequencies

A transducer mounted in a large baffle provides, at low frequencies $f < f_s$, the efficiency

$$\eta(f < f_s) \approx \frac{(Bl)^2 S_D^2}{R_E K_{MS}^2} \frac{\rho_0 2\pi f^2}{c} \qquad (7)$$

and the voltage sensitivity:

$$SPL_{u_{ref}, r_{ref}}(f < f_s) \approx 20\lg\left(\frac{\rho_0 Bl S_D 2\pi f^2}{|r_{ref}| R_E K_{MS}} \frac{u_{ref}}{p_0} \right) \qquad (8)$$

Both characteristics rise with the frequency squared, whereas force factor Bl and resistance R_E have the same influence as in the passband. A lower stiffness K_{MS} of the suspension would increase the efficiency and sensitivity in this frequency band.

Table 1: Optimization of efficiency

Application	**Maximize in Transducer Design**	**Design Rules**
A1: Full band loudspeaker using sealed, vented box or passive radiator system ($f_0/2 < f$)	$\frac{Bl^2}{R_E}\frac{1}{M_{MS}^2}$	D2, D4-D7
A2: Woofer using small closed-box, vented-box or passive radiator system ($f < 2f_0$)	$\frac{Bl^2}{R_E}$	D3, D4-D7
A3: Subwoofer in large sealed-box ($f_0/3 < f < 2f_0$)	$\frac{Bl^2}{R_E K_{MS}^2}$	D3, D4-D7, D9
A4: Narrow-band subwoofer in sealed-box system ($0.75f_0 < f < 1.25f_0$)	$\frac{1}{R_{MS}}$	D11-D13
A5: Woofer with bandpass system ($f_p/2 < f < 2f_0$)	$\frac{Bl^2}{R_E}$	D3, D4-D7
A6: Micro-speaker with small rear volume and side-fire port ($f_0 < f < 2f_p$)	$\frac{Bl^2}{R_E}\frac{1}{(M_{MS}+M_{MP})^2}$	D2, D4-D7
A7: Flat panel with exciter ($f_0/2 < f$)	$\frac{Bl^2}{R_E}\frac{1}{M_{MS}^2}$	D2, D4-D7

3 Transducer Requirements

The previous discussion shows that the effective radiation area S_D increases efficiency $\eta(f)$ and voltage sensitivity $SPL_{1V,1m}(f)$ at all frequencies in the same way. This is only true for the transducer mounted in the baffle, but S_D may change the frequency responses $\eta(f)$ and $SPL_{1V,1m}(f)$ if the transducer drives additional acoustical elements (e.g. closed box). Finding the optimal radiation size S_D is an important step in the system design, see section 7.2 in [2], but is less relevant for transducer optimization discussed here.

The other lumped transducer parameters R_E, R_{MS}, Bl, M_{MS} and K_{MS} determine the frequency dependency of $\eta(f)$ and $SPL_{1V,1m}(f)$ and the interaction with voltage spectrum $G_U(f)$ generating the efficiency η and $SPL_{1V,1m}$ when a broadband audio signal is reproduced.

Thus, the optimization of the transducer also depends on the voltage spectrum $G_U(f)$ and the load impedance $Z_L(f)$ of the mechano-acoustical system. If the system design requires an improvement of transducer efficiency $\Delta\eta/\eta$ and voltage sensitivity ΔSPL as defined in Eqs. (43) and (44) in [2], it is useful to focus the optimization on the lumped transducer parameters that have the highest influence in the particular application.

Table 2: Optimization of voltage sensitivity

Application	**Maximize in Transducer Design**	**Use Design Rules**
A1: Full band loudspeaker using sealed, vented box or passive radiator system ($f_0/2 < f$)	$\frac{Bl}{R_E}\frac{1}{M_{MS}}$	D1, D2, D4-D7
A2: Woofer using small closed-box, vented-box or passive radiator system ($f < 2f_0$)	$\frac{Bl}{R_E}$	D1, D3, D4-D7
A3: Subwoofer in large sealed-box ($f_0/3 < f < 2f_0$)	$\frac{Bl}{R_E K_{MS}}$	D1, D3, D4-D7,D9
A4: Narrow-band subwoofer in sealed-box system ($0.75f_0 < f < 1.25f_0$)	$\frac{1}{Bl}$	D10-D13
A5: Woofer with bandpass system ($f_p/2 < f < 2f_0$)	$\frac{Bl}{R_E}$	D1, D3, D4-D7
A6: Micro-speaker with small rear volume and side-fire port ($f_0 < f < 2f_p$)	$\frac{Bl}{R_E}\frac{1}{(M_{MS}+M_{MP})}$	D1, D3, D4-D7
A7: Flat panel with exciter ($f_0/2 < f$)	$\frac{Bl}{R_E}\frac{1}{M_{MS}}$	D1, D2, D4-D7, D16-D21

The tables 1 and 2 illustrate the parameter ratio for seven applications (A1-A7) that should be maximized in the transducer design to improve power efficiency and voltage sensitivity, respectively. The right column gives a reference to practical design considerations (D1-D20) listed in Table 3.

It is beneficial to maximize the motor efficiency factor $(Bl)^2/R_E$ in such applications where a high force

is required for driving the load of the mechano-acoustical system coupled to the transducer [11]. The moving mass M_{MS} shall be minimized, while keeping the efficiency factor $(Bl)^2/R_E$ as high as possible, in all applications (A1, A6, A7), where the transducer is operated dominantly in the passband region and the crossover frequency is high ($f_{XO} >> f_0$).

Only in a particular application (A4) such as a subwoofer operated in a narrow band ($0.75f_0 < f < 1.25f_0$) would a low mechanical resistance R_{MS} and a weak motor with low force factor Bl provide more efficiency and voltage sensitivity [10].

Table 3: Design considerations for improving efficiency and sensitivity in system design

	Optimal Design Considerations
D1	Shorten wire length and increase diameter to reduce DC resistance R_E while keeping the same motor efficiency factor Bl^2/R_E
D2	Use aluminum coil wire to reduce moving mass M_{MS}
D3	Use copper coil wire to improve motor efficiency factor Bl^2/R_E
D4	Use coil height $h_{coil} \approx 2X_{max}$ to keep 50 % of the windings in the gap at maximum excursion X_{max}
D5	Keep magnetic fringe field outside gap as small as possible
D6	Use small voice coil overhang to exploit the fringe field
D7	Use nonlinear force factor $Bl(x)$ to reduce electrical damping at higher amplitudes
D8	Reduce effective radiation area S_D
D9	Use soft suspension in the intended working range $x < X_{max}$ (not progressive $K_{MS}(x)$ dependency)
D10	Reduce airflow in the gap to decrease R_{MS}
D11	Reduce losses in suspension to decrease R_{MS}
D12	Use mass and stiffness to tune the cut-off frequency fc of the loudspeaker
D13	Use a small magnet to reduce electrical damping
D14	Use absorbing filling in the rear enclosure
D15	Shorten and widen the side-fire port to reduce acoustical mass M_{AP}
D16	Increase the number and density of vibrations modes
D17	Place the actuator at the optimal excitation point $\mathbf{r}_e$
D18	Clamp the exciter or use a higher magnet mass M_{mag}
D19	Reduce the moving mass M_{MS} of the exciter
D20	Generate a mode shape that minimizes acoustical cancellation
D21	Use a lower damping ratio for the radiator material (cone, panel)

4 Transducer Design

After presenting the fundamental relationships between efficiency and lumped transducer parameters, this section discusses the influence of the geometry, choice of the material and other design considerations.

4.1 Gap-Coil Topology

For an electro-dynamical transducer, the relationship between the gap depth h_g and the voice coil height h_c is a good starting point in our search for maximum efficiency in sound reproduction.

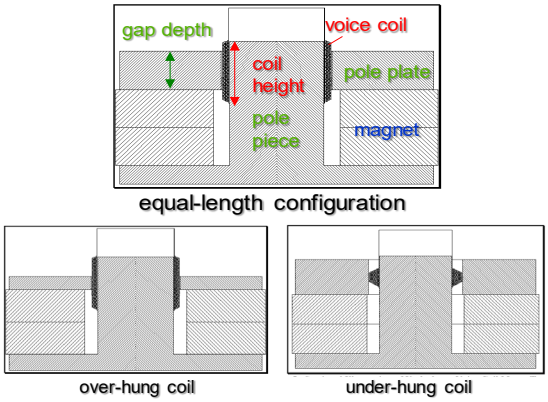

Figure 3: Common topologies for configuring the gap-depth and voice coil height in electro-dynamical transducers

Figure 3 shows typical configurations to maximize either efficiency or linearity of the electro-dynamical transducer. The so-called equal-length configuration uses a minimum voice coil overhang to exploit the magnetic fringe field outside the gap. This configuration gives the highest force factor value $Bl(x=0)$ at the voice coil rest position, which is beneficial for maximizing the effective force factor $\overline{Bl}$ when reproducing common audio signals at high amplitudes (as discussed in [2]).

Unfortunately, the equal-length configuration without nonlinear control generates significant harmonic and intermodulation distortion and other undesired nonlinear symptoms (DC-displacement, instabilities…) at larger voice coil displacement x [12]. Figure 4 shows the nonlinear force factor characteristic $Bl(x)$ calculated by a magnetic finite element model where the gap depth h_g was varied between 5, 10, 15 and 20 mm while assuming the coil height h_c=10 mm and magnet size are constant [13].

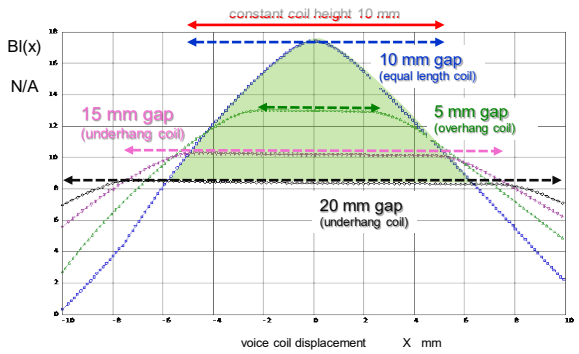

Figure 4: Force factor $Bl(x)$ versus displacement x of an equal-length, an overhung and an underhung configurations using a constant voice coil height and different gap depths.

The overhung configuration shown in Figure 3 uses spare windings below and above the gap that are used when the voice coil is moved. This generates a plateau in the $Bl(x)$ characteristic ($h_g = 5$ mm in Figure 4), giving more linearity and less nonlinear distortion for moderate excursion.

The underhung configurations in Figure 4 use 15 and 20 mm thick pole plates to generate a wider linear plateau in the nonlinear $Bl(x)$ characteristics.

The price paid for less $Bl(x)$-variation and lower nonlinear distortion is a loss of force factor, illustrated as shaded area in Figure 4.

Topology	**Equal-length**	**Over-hang**	**Under-hang**
Motor efficiency factor $\overline{Bl}^2 / R_E$	High	low	low
Moving mass M_{MS}	medium	high	low
$Bl(x)$-nonlinearity	Strong	weak	weak
$L(x)$-nonlinearity	medium	strong	weak
DC-Stability	critical	robust	robust
Weight, size cost	Low	medium	high

Table 4: Overview of benefits and drawbacks of selected motor topologies using different ratios between voice coil height and depth length

Table 4 summarizes the properties of the common motor topologies. The equal-length configuration has been used for consumer applications where maximum output, efficiency, cost, size and weight require a compromise in linearity. The overhung configuration is attractive for subwoofer applications where the moving mass and inductance nonlinearities $L(x)$ and $L(i)$ are less important. The underhung coil is an interesting topology for all high-frequency applications (e.g. tweeter) where the coil mass limits the overall efficiency. While both the overhung and underhung configurations are relatively robust to an offset of the voice coil rest position caused by production variances and aging, the equal-length configuration is sensitive to an offset and may generate a significant DC displacement by rectifying the AC audio signal.

Nevertheless, the equal-length configuration is the best candidate for active systems where the passive transducer provides the highest efficiency over a wide audio band and digital signal processing can be used to cancel the nonlinear loudspeaker distortion [4] and actively stabilize the voice coil position [7]. For this reason, the remaining parts of this section focus on the optimal design of the equal-length configuration.

4.2 Motor Efficiency Factor

The efficiency at low frequencies and in the passband in Eqs. (1) and (7) depends on the squared effective force factor divided by the DC resistance, which can be interpreted as a motor efficiency factor $(Bl)^2/R_E$.

Expressing DC resistance as

$$R_E = \rho_E \frac{l}{A_w} = \rho_E \frac{l^2}{V_w} \qquad (9)$$

with the length l, cross-sectional area A_w and the electrical resistivity ρ_E of the wire, and neglecting the magnetic fringe field outside the gap allows the motor efficiency factor to be written as

$$\frac{(Bl)^2}{R_E} = \overline{B}^2 \frac{V_w}{\rho_E} \qquad (10)$$

using $\overline{B}^2$ to represent the mean induction seen by the conductive wire material of the volume V_w. Eq. (10) shows that the motor efficiency factor is independent of the length l and cross-sectional area A_w of the wire. This fact gives the loudspeaker designer some freedom in realizing the desired voltage sensitivity, as discussed in section 5, by trading force factor Bl against DC resistance R_E.

The volume V_w can be increased by maximizing the fill factor in the coil winding area [14] by using rectangular wire and an efficient winding layout, which usually increases the manufacturing effort and cost. In practice, there is not much freedom to increase volume V_w by using a thinner bobbin material and reducing the clearance in the gap, which is required to cope with rocking modes and voice coil rubbing.

Material	**Resistivity ρ_E**	**Density ρ_D**
Copper	1.68×10^{-8} Ωm	8.96 g/cm^3
Aluminum	2.65×10^{-8} Ωm	2.7 g/cm^3

Table 5: Resistivity and density of common wire material

4.3 Coil Material

The electrical resistivity ρ_E and the density ρ_D of the wire material given in Table 5 affect the DC resistance R_E and the total moving mass M_{MS}, respectively.

This has a significant influence on the passband efficiency

$$\eta_{PB} = \frac{\overline{B}^2 V_w}{\rho_E \left(\rho_D V_w + M_{add}\right)^2} \frac{\rho_0 S_D^2}{2\pi c} \qquad (11)$$

considering the additional mass M_{add}, representing the contribution of other moving loudspeaker parts such as suspension, diaphragm, bobbin and moving air.

Choosing the volume V_w and the proper material of the wire depend on the ratio between additional mass and coil mass:

$$M_{ratio} = \frac{M_{add}}{\rho_D V_w} \qquad (12)$$

If the mass ratio $M_{ratio} >> 1$, a larger wire volume V_w increases the passband efficiency. Using copper instead of aluminum as coil wire would increase the passband efficiency η_{PB} by half if the coil mass is negligible compared to the total mass M_{MS} because aluminum has a higher resistivity. If the mass ratio $M_{ratio} << 1$ and the coil mass dominates the total moving mass M_{MS}, an aluminum coil provides 6 times more passband efficiency than a copper coil.

4.4 Voice Coil Height

The voice coil height h_c limits the maximum displacement X_{Bl} in an equal-length configuration. According to IEC standard 62458 [15], the force factor $Bl(X_{Bl})$ referred to the force factor value at the rest position $Bl(x=0)$ drops at the peak displacement X_{Bl} to a given force factor ratio Bl_{min}:

$$\min_{-X_{Bl}<x<X_{Bl}} \left(\frac{Bl(x)}{Bl(0)} \right) \cdot 100\% = Bl_{\min} \qquad (13)$$

For example, moving the coil to a force factor ratio Bl_{min} = 82 % generates about 10 % inter-modulation distortion for a two-tone signal [16]. If nonlinear control can be applied to the loudspeaker and the nonlinear distortion can be actively canceled, the force factor ratio can be reduced to Bl_{min} = 50 %, giving a larger maximum displacement $X_{Bl} \approx h_c/2$. At this point, half of the coil is out of the gap if the fringe field is small and there is no offset in the voice coil rest position.

Theoretically, the nonlinear control could be applied to even larger peak displacements where the force factor ratio is much lower but the compensation of the $Bl(x)$ distortion would increase the crest factor CF_u of the pre-distorted signal, which has to be provided by the power amplifier. Exploiting peak displacement where the force factor ratio Bl_{min} decays to 50% is a good compromise for active linearization of a loudspeaker reproducing common (broadband) audio signals with a Gaussian-like probability density function $pdf(x)$ [2]. In this case, there is no increase in power consumption and only a moderate increase in peak voltage requirement.

4.5 Gap Depth

After defining the voice coil height h_c, the optimal gap depth h_g shall be determined in order to exploit the magnetic fringe field outside the gap. The induction B within the gap and in the fringe field, as illustrated in Figure 5, can be calculated by using a magnetic finite element simulation tool.

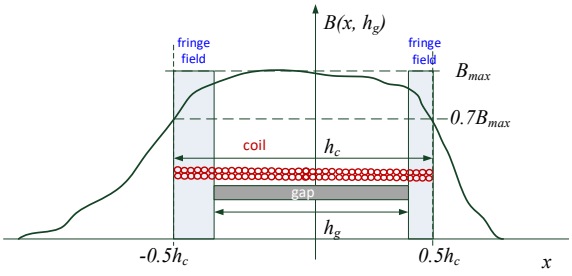

Figure 5: Voice coil overhang exploits the magnetic fringe field in the magnetic induction $B(x, h_g)$ outside the magnetic gap with the gap depth h_g.

The optimal value h_g for maximizing the motor efficiency factor can be found by a gap geometry at which the induction at both ends of the voice coil

$$B(x = \pm 0.5 h_c, h_g) = 0.7 B_{\max} \qquad (14)$$

is 70% of the maximum induction B_{max} in the gap. For a smaller value of the gap depth h_g, the windings at both ends of the voice coil would generate a lower contribution to the squared Bl value while increasing the electrical resistance R_E, giving a lower motor efficiency factor Bl^2/R_E.

4.6 Magnet Geometry

After defining the clearance between the voice coil and the pole plates, the gap width w_g and the pole plate surface A_g can be determined, giving the gap volume $V_g = A_g w_g$. In order to generate the highest induction B_g in the gap, the optimal working point in the demagnetization curve shown in Figure 6 must be used.

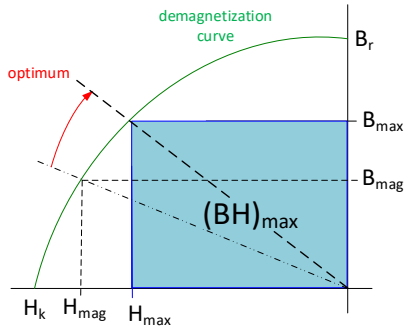

Figure 6: Optimal working point in the demagnetization curve of the magnet.

The induction B_{mag} and field strength H_{mag} in the magnet should be close to the optimal values B_{max} and H_{max}, giving the maximum product

$$Max\left(B_{mag}H_{mag}\right)\overset{!}{=}B_{\max}H_{\max}=\left(BH\right)_{\max} \tag{15}$$

with the maximum energy product $(BH)_{max}$, which is an important material parameter of the magnet.

Neglecting the iron in the pole piece and plates, the maximum value of the induction in the gap for a given magnet volume $V_m=h_mA_m$ can be estimated by

$$B_g=\sqrt{\frac{\mu_0\left(BH\right)_{\max}V_m}{V_g}}\,. \tag{16}$$

This value can be realized if the magnet height

$$h_m=\frac{B_g w_g}{\mu_0 H_{\max}} \tag{17}$$

and the cross-sectional area

$$A_m=\frac{B_g A_g}{B_{\max}} \tag{18}$$

correspond to the gap width w_g and the pole plate surface A_g of the gap. Modern finite element magnetic simulation tools simplify this optimization process while considering the saturation of the iron material and the fringe field outside the gap.

4.7 Suspension

The total stiffness K_{MS} in the denominator in Eq. (7) reduces the efficiency and voltage sensitivity at frequencies below resonance. It would be desirable to further reduce the transversal stiffness K_{MS} while ensuring an optimal voice coil rest position, keeping enough radial stiffness K_{rad} to center the coil in the gap and sufficient rotational stiffness to suppress rocking modes generating voice coil rubbing [17]. This is important for flat loudspeakers where the distance between spider and surround is small or in headphones, micro-speakers, compression drivers and other transducers in which no spider is used.

However, a mechanical suspension becomes softer during the product life due to break-in, climate and fatigue in the rubber, fabric, foam and suspension materials. Mechanical overload may also speed up the natural aging process [18]. External forces generated by gravity and a static air pressure difference between front and rear side of the diaphragm (e.g. as caused by the air stream in cars when a window is open) may also change the voice coil position. This is critical in transducers with an equal-length configuration, where a small coil offset leads to a significant asymmetry in the $Bl(x)$-nonlinearity.

Asymmetries in the loudspeaker nonlinearities also generate a DC force that works against the mechanical stiffness $K_{MS}(x=0)$. If the mechanical suspension is too soft, a significant DC displacement might be generated, leading to bifurcation and other unstable behavior as well as excessive distortion [12].

The surround is the most critical part in loudspeakers because voice coil displacement and air pressure in the rear enclosure generate significant deformation, which also affects the modal vibration at higher frequencies [2].

Adaptive nonlinear control can cope with those problems. Active stabilization [7] and distortion cancelation [4] keep the voice coil at the optimal voice coil rest position and ensure maximum AC displacement and sound pressure output. An active protection system [6] more reliably prevents an overload and provides more output than a suspension with a progressive stiffness characteristic.

5 Optimizing Voltage Sensitivity

The voltage sensitivity is a useful characteristic to decide whether the peak voltage capabilities of the power amplifier are sufficient to generate the target SPL output at all frequencies of interest.

It is possible to modify the voltage sensitivity without significantly degrading the efficiency, which was the primary design goal so far. For example, changing the DC resistance R_E of the voice coil while maintaining the same motor efficiency factor $(Bl)^2/R_E$ will not change the efficiency $\eta(f)$ in Eqs. (1), (4) and (7) as long as the volume V_C of the wire material is constant. The difference in the voltage sensitivity of two designs with only different DC resistances R_E and R_E' becomes:

$$\begin{aligned}&SPL_{u_{ref},r_{ref}}(f)\Big|_{R_E}-SPL_{u_{ref},r_{ref}}(f)\Big|_{R_E'}\\&=10\lg\left(\frac{R_E'}{R_E}\right)\end{aligned} \tag{19}$$

Practically speaking, reducing the DC resistance to half of its value gives 3dB more voltage sensitivity.

6 Amplification

The power amplification (amplifier, power supply, cables, …) uses critical hardware components that determine the size, energy consumption, heat development and cost of the product. The long-term maximum output power is the most popular characteristic of the amplifier. It is usually measured by using a sinusoidal test signal (e.g. chirp) and a resistor corresponding to the nominal impedance Z_N of the transducer [19]. The long-term power capability of the amplifier is usually not a limiting factor for a common audio signal (e.g. music) where the crest factor (CF_u > 12 dB) is much higher than for a sinusoidal signal (CF_u = 3dB) and where the transducer has a complex and frequency dependent input impedance $Z_E(f)$ [20]. The back EMF and the voice coil inductance L_E reduce the voltage sensitivity, especially in efficient transducers having a high motor efficiency factor $(Bl)^2/R_E$ see Figure 2.

Reducing the DC resistance R_E of the coil is a practical solution but requires shorter cables and a low output impedance of the power amplifier. However, reducing R_E will increase the current and the heating of the amplifier output stage. Even if the amplifier can provide the RMS current and long-term power to the speaker, the high crest factor of common audio signals generates high current peaks which may lead to a critical temperature in the amplifier output stage after a short time [21].

Thus, the thermal protection of the amplifier is a similar problem to the thermal protection of the voice coil in the transducer, although there are significant differences in the heat flow, the cooling mechanisms and the thermal time constants.

Combining the protection of both FET output stage and coil in a common control block would improve the maximum short-term power capacity of the amplifier.

7 Case Study

The freedom provided by nonlinear adaptive control shall be illustrated using an existing 4.5" woofer **A** developed for automotive applications. A minor modification has been performed in transducer **B** by shorting the voice coil to half of the height found in the original transducer **A** while using the same coil wire, magnetic system, suspension and diaphragm. This change did not increase the cost and was accomplished without redesigning the motor structure. Although the modified transducer **B** has not been optimized to the maximum efficiency, this small modification improves the total performance of the transducer with nonlinear control significantly.

Transducer Parameters	**A**	**B**	Change
Nominal impedance [Ω]	4	2	-50%
Gap depth d_g [mm]	5	5	0%
Coil height h_c [mm]	11	5.75	-47%
Resistance R_E[Ω]	3.31	1.74	**-47%**
Force factor $Bl(0)$ [N/A]	4.6	3.5	**-24%**
Bl limited peak displacement X_{Bl} [mm]	4.5	3.5	**-40%**
Motor efficiency factor $Bl(0)^2/R_E$[Ns/m]	6.39	7.04	**+10%**
Compliance C_{ms} [mm/N]	0.66	0.67	+1%
Moving mass M_{MS} [g]	10.4	8.6	**-17%**
Mass ratio M_{ratio}	1.5	3	+100%
Resonance frequency f_s [Hz]	61	67	+10%
Passband efficiency η_{PB} [%]	0.267	0.433	**+62%**
Voltage sensitivity in passband $SPL_{PB,1Vrms,\ 1m}$ [dB]	81.2	85.9	**+4.7dB**

Table 6: Characteristics of the original transducer (**A**) and the optimized transducer (**B**) with reduced voice coil height h_c.

8 Transducer Characteristics

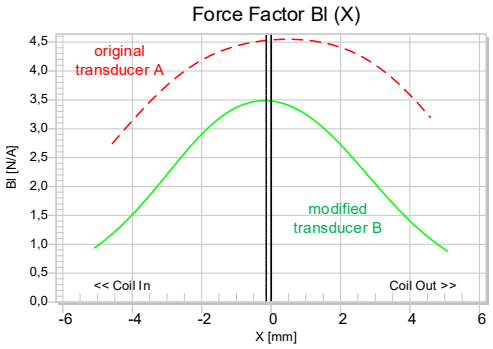

Figure 7: Force factor characteristic $Bl(x)$ of the original speaker A with an overhung configuration (dashed line) and the modified speaker B with an equal-length configuration (solid line).

Figure 7 s*hows that the original transducer **A** with voice coil overhung of 6 mm almost has a plateau region where the force factor Bl(x) is constant for small displacement |x| < 3 mm. A significant fringe field outside the gap also gives 24 % more force factor Bl(x=0) at the rest position than the modified speaker **B** with the shorter coil height* $h_c \approx h_g$. *The shorter coil height causes an earlier decay in the* Bl*(x)-nonlinearity and already generates 10 % IM-distortion at Bl-limited peak displacement* X_{Bl} = 3.5

mm [15]*. However, the reduced DC resistance R_E= 1.74 Ω leads to a 10 % higher motor efficiency factor Bl^2/R_E in the modified speaker* ***B****. The same improvement can be found in the efficiency $\eta(f<f_s)$ below resonance.*

The motor efficiency factor can be further optimized by a slightly longer coil $h_c \approx 7$ mm to exploit the fringe field according to the condition specified in Eq. (17)*. A motor design tool based on magnet FE analysis can be used to the find the optimal voice and wire dimensions giving the nominal impedance of 2 Ω.*

The shorter coil in the modified transducer ***B*** *reduces the total moving mass M_{MS} by 17%.* This shifts the resonance frequency f_s up slightly because the stiffness of the suspension has not been changed significantly. *Since the mass ratio M_{ratio} is larger than 1, the reduction of the voice coil mass still has a large influence on the passband efficiency. Combined with the improved motor efficiency factor Bl^2/R_E,* the pass-band efficiency η_{PB} is increased by 62% in the modified transducer **B**.

The passband voltage sensitivity $SPL_{PB,1Vrms,1m}(f>f_s)$, which determines the peak voltage demands of the amplifier, is about 5 dB higher in the modified speaker **B** with 2 dB contribution from improved efficiency and almost 3 dB from the reduced DC resistance R_E.

The optimal use of the system resources will be illustrated by comparing the performance of two closed-box systems using an original woofer (**A**) and a modified woofer (**B**), each mounted in a 1.6 liter sealed enclosure and operated below a crossover frequency at 1.5 kHz.

Both closed-box systems are evaluated by linear and nonlinear control schemes based on the KCS-technology [22] with voltage and current monitoring which have been implemented in a micro-controller *ARM M4*. Both control schemes equalize the overall transfer response and generate the same 6th-order Chebyshev alignment to a cut-off frequency fc=100 Hz.

Only the nonlinear control (+**NC**) stabilizes the voice coil position, compensates for harmonic and intermodulation distortion and generates a linear relationship between control input and sound pressure output. The nonlinear control system also provides reliable mechanical and thermal protection and attenuates the input signal if the peak displacement would exceed x_{prot} =3.5 mm or if the voice coil temperature would rise more than ΔT_{prot}=130 K.

The linear control (+**LC**) cannot cope with the compression of the fundamental, nonlinear distortion, DC displacement and other nonlinear effects at higher amplitudes. Therefore, linear control needs a larger safety margin in the mechanical protection due to the uncertainties in the voice coil position.

8.1 Audio Performance

A typical music stimulus (*Tracy Chapman, Crossroads, This Time*) has been used to evaluate the performance of the original (**A**) and modified (**B**) loudspeaker with linear (+**LC**) and nonlinear control (+**NC**). The magnitude of music stimulus is adjusted at the control input of all four active loudspeaker systems listed in Table 7 to produce a total SPL ≈ 92 dB at a distance of r=0.1m.

Active Speaker Characteristics	**A +LC**	**B +LC**	**A +NC**	**B +NC**
SPL [dB]	91.8	92.1	92.2	92.2
Displacement peak X_p [mm]	3.3	3.4	3.2	3.3
Displacement rms X_{ac} [mm]	0.51	0.53	0.51	0.54
Crest factor CF_X [dB]	16.1	16.1	15.9	15.9
Distortion Compensation *EID* [%]	-	-	11	30 (+19%)
Voltage peak U_p [V]	45.5	26.8	45.6	30.4 (-33%)
Voltage rms U_{ac} [V_{rms}]	8.7	4.7	8.7	4.7 (-45%)
Crest factor CF_u [dB]	14.3	15.1	14.3	16.2
Real input power P_e [W]			14.2	8.4 (-40%)
Temperature coil ΔT_v [K]			+96	+59 (-39%)

Table 7: Performance of the original loudspeaker (**A**) and the modified speaker (**B**) with linear control (+**LC**) and nonlinear control (+**NC**) while reproducing a typical audio signal.

The four active speakers generate similar sound pressure spectra and almost the same rms and peak displacement, giving a crest factor CF_x of 16 dB, which is typical for common audio signals. Thus, most of the time, the coil stays in the gap, and the effective force factor $\overline{B}$ is nearly equal to the maximum $Bl(x=0)$ at the rest position, as predicted in the first part of this paper [2] for most audio signals having a Gaussian $pdf(x)$.

For the linearization of the original speaker (**A+NC**), the nonlinear control generates additional compensation distortions that are 11 % of the peak value of the terminal voltage and correspond to the equivalent input distortions (*EID* [23]) generated by the loudspeaker. The small compensation signal does not increase the crest factor in the pre-distorted input signal. However, the linearization of the modified speaker (**B+NC**) requires a three times larger peak value of the compensation distortion, which increases

the crest factor of the input signal by about 1 dB compared to linear control (**B+LC**). However, this increase is similar to the effect of the equalization at low frequencies. The different alignment of the original and modified speaker (**A+LC**) and (**B+LC**) generates an increase of the crest factor in the terminal voltage by 0.5 dB and 1.3 dB, respectively, due to the difference in the transducer resonance frequency f_s in free air. This increase is caused by boosting low-frequency components having a higher crest factor ($CF_x \approx 16$ dB) than the full band audio signal.

This small increase in the crest factor can easily be compensated by the much better voltage sensitivity of the modified speaker with nonlinear control **B+NC** compared to the original speaker **A+NC,** which reduces the peak voltage requirement for the amplifier by 33 %.

The shorter coil in the modified speaker under nonlinear control (**B+NC**) reduces the power consumption and the heat development by 40%. This transducer operated with reliable active protection (**B+NC**) can generate at least 3 dB more SPL (measured as a total mean value over the stimulus) by requiring less peak voltage than in the original speaker **A+NC**.

Exploiting the full voltage capability provided by the amplifier, the mechanical protection system in the modified speaker **B+NC** would reduce the bass signal ($f < f_s$) by 3 dB to keep the peak excursion below x_{prot} = 3.5 mm. The 3 dB increase of SPL would require 17 W of real input power and would heat up the voice coil temperature by $\Delta T_v \approx 120$ K, which would be permissible for the speaker **B**. Doubling the electric input power provided to the original speaker **A** would not only require a more powerful amplifier but would also generate an unacceptable increase of the coil temperature $\Delta T_v \approx 200$ K.

8.2 Distortion Reduction

Figure 8 *shows the active compensation of the harmonic distortion generated by a single excitation tone. Since the modified transducer **B** is carefully manufactured, the 2nd-order distortion found under linear control is relatively small, indicating symmetrical stiffness $K_{MS}(x)$ and force factor $Bl(x)$ characteristics. The nonlinear control **NC** is required for speaker **B** to reduce the high value (40 %) of 3rd-order harmonic distortion by 20 dB at low frequencies.*

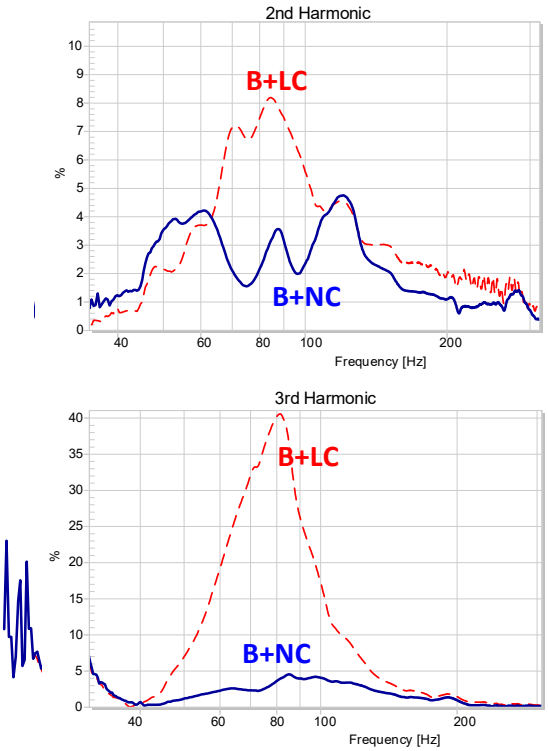

Figure 8: 2nd- and 3rd order harmonic distortion of the optimized loudspeaker with linear control (**B+LC**) and nonlinear control (**B+NC**).

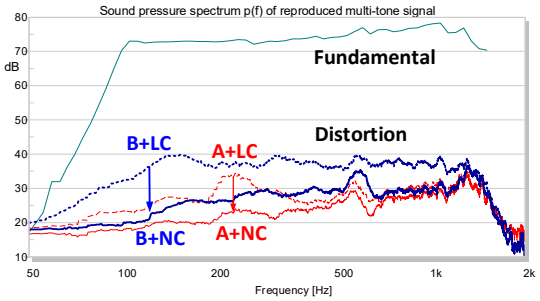

Figure 9: Fundamental components and nonlinear distortion in a multi-tone test stimulus reproduced by the original loudspeaker (**A**) and the modified loudspeaker (**B**) with linear (+**LC**) and nonlinear control (+**NC**).

The nonlinear control (+**NC**) also reduces the intermodulation distortion generated by a more complex stimulus (e.g. music) as shown for a sparse multi-tone stimulus in Figure 9. The distortion reduction achieved for the original speaker **A+NC** and modified speaker **B+NC** are shown as thin solid and thick solid lines, respectively, while the dashed lines represent the nonlinear distortion found with linear control **LC**.

The modified speaker with linear control **B+LC** generates much higher distortion than the original

speaker **A+LC**, but nonlinear control can reduce the distortion by more than 15 dB at low frequencies. Here, the nonlinear motor with nonlinear control **B+NC** generates lower distortion than the original speaker **A+LC** that uses a much more linear motor. At 600 Hz and 1.3 kHz, there are nonlinear modal vibrations on the cone which cannot be canceled by the control structure, which is based on lumped parameter modeling.

9 Conclusions

Assigning a higher priority to the efficiency than to the linear and nonlinear distortion generated in the electro-acoustical conversion changes the paradigm in transducer design. A small voice coil overhang generating a significant force factor nonlinearity leads to a stronger motor and a lighter coil than a linear motor design. Other design choices with a smaller magnet, simplified suspension or transducer without shorting rings reduce the size, weight and cost of product but also generate more distortion which can be cancelled by nonlinear control. Active stabilization of the voice coil rest position in combination with a reliable protection system applied to a softer, less progressive suspension gives more peak displacement and better bass performance.

The voltage sensitivity of transducer is the second most important characteristic because it is important for selecting an amplifier with sufficient peak voltage and current capabilities.

For electro-dynamical loudspeakers with a high motor efficiency factor $(Bl)^2/R_E$, a lower DC resistance ($R_E \leq 2\ \Omega$) would be beneficial for common audio signals (e.g. music) with a high crest factor but requires proper tinsel leads and short cables between transducer and amplifier.

Placing the power amplification closer to transducer or especially integrating both components in one active transducer module will not only solve the cable problems but allows for simplification of the output filter in Class D amplifiers while fulfilling the EMC requirements. The module should also include the current sensor, the adaptive nonlinear controller and the amplifier and an interface for modern audio streaming [24]. This smart transducer module simplifies and speeds up the development of complete audio systems and provides valuable diagnostic information over the life time of the product.

The new approach in Green Speaker Design illustrated for an electro-dynamical transducer and selected mechano-acoustical systems can also be applied to other transducer types (e.g. piezo-ceramic) and other acoustical systems (e.g. horn, transmission line).

10 References

[1] R. Small, “Direct Radiator Loudspeaker System Analysis,” J. Audio Eng. Soc. 1972, vol. 20, no. 5, pp. 307-327.

[2] W. Klippel, “Green Speaker Design (Part 1: Optimal Use of Transducer Resources),” presented 146th Convention of Audio Eng. Soc., Dublin, Ireland, 2019 March 20–23.

[3] W. Klippel, “Nonlinear Adaptive Controller for Loudspeakers with Current Sensor,” presented at the 106th Convention of the Audio Eng. Soc., Munich, May 1999, preprint 4864.

[4] W. Klippel, "The Mirror Filter - a New Basis for Reducing Nonlinear Distortion Reduction and Equalizing Response in Woofer Systems", J. Audio Eng. Soc., vol. 32, no. 9, pp. 675-691, (1992).

[5] K. M. Pedersen, “Thermal Overload Protection of High-Frequency Loudspeakers,” Rep. of final year dissertation, Salford University, UK (2002).

[6] W. Klippel, “Mechanical Overload Protection of Loudspeaker Systems,” J. Audio Eng. Soc., vol. 64, no. 10, pp. 771 – 783 (October 2016).

[7] W. Klippel, “Adaptive Stabilization of Electro-dynamic Transducers,” J. Audio Eng. Soc. vol. 63, no. 3 pp. 154-160, (March 2015).

[8] L. Beranek, T. Mellow, “Acoustics: Sound Field and Transducers,” Academic Press, Amsterdam.

[9] D. B. Keele, “Maximum Efficiency of Direct Radiator Loudspeakers,” presented at the 91st Convention of the Audio Eng. Soc., preprint no. 3193 (Oct. 1991).

[10] R. Aarts, “High-efficiency low-Bl loudspeakers,” J. Audio Eng. Soc. vol. 53, pp. 579–592 (2005).

[11] J. Vanderkooy, P. Boers, and R. Aarts, “Direct-Radiator Loudspeaker Systems with High Bl,” J. Audio Eng. Soc., vol. 51, no. 7/8 (July/August 2003).

[12] W. Klippel, “Loudspeaker Nonlinearities – Causes Parameters, Symptoms,” J. Audio Eng. Soc. 54, no. 10, pp 907 – 939 (Oct. 2006).

[13] M. Dodd, personal communication.

[14] N. E. Iversen, et. al. “Relationship between Voice Coil Fill Factor and Loudspeaker Efficiency,” J. Audio Eng. Soc., vol. 64, no. 4, pp. 241-252 (April 2016).

[15] IEC 62458:2010 Sound System Equipment – Electro-acoustical Transducers – Measurement of Large Signal Parameters

[16] W. Klippel, “Assessment of Voice-Coil Peak Displacement Xmax”, J. Audio Eng. Soc. vol. 51, no. 5, pp. 307-324 (May, 2003).

[17] W. Cardenas, W. Klippel, “Root Cause Analysis of Rocking Modes,” J. Audio Eng. Soc., vol. 64, no. 12, pp. 969-977, (December 2016).

[18] W. Klippel, “Mechanical Fatigue and Load-Induced Aging of Loudspeaker Suspension,”

presented at the 131st Convention of Audio Eng. Soc. 2011, Oct. 20-23, NY, USA
[19] W. M. Leach," Introduction to Electroacoustics and Audio Amplifier Design", Kendall/Hunt Publishing Company, 2003.
[20] N. E. Iversen, et. al., "Efficiency Investigation of Switch-Mode Power Audio Amplifiers Driving Low Impedance Transducers", presented at the 139th convention of Audio Eng. Soc., New York, 2015, preprint 9377.
[21] S. Poulsen and M. A. E. Andersen, "Practical Considerations for Integrating Switch Mode Amplifiers and Loudspeakers for a Higher Power efficiency", presented at the 116th convention of Audio Eng. Soc., Berlin, 2004, preprint 6155.
[22] Klippel Controlled Sound (KCS), Klippel GmbH, www. klippel.de
[23] IEC 60268-21: Sound System Equipment – Part Acoustical (Output Based) Measurements, draft 2017
[24] J. Boehm, "A distributed Audio System for Automotive Applications," Presented at the 144th Convention of the Audio Eng. Soc., Milano, 2004, e-Brief #450.